PHYSICAL REVIEW B VOLUME 33, NUMBER 12 15 JUNE 1986

Quantitative analysis of streaks in reflection high-energy electron diffraction: GaAs and AlAs deposited on GaAs(001)

C. S. Lent* and P. I. Cohen
Department of Electrical Engineering, University of Minnesota, Minneapolis, Minnesota 55455
(Received 25 June 1985; revised manuscript received 6 January 1986)

Reflection high-energy electron diffraction (RHEED) has long been considered a qualitative tool for assessing the roughness of a surface and for determining whether thin films are deposited epitaxially. Though this technique is known to be exceedingly surface sensitive, no quantitative statements could be made. In this paper we report measurements of the specular diffraction beam from near-singular GaAs(001) surfaces with submonolayer deposits of GaAs and AlAs. By fitting the shapes of these beams to a kinematic calculation, exact to within the column approximation, we determine the coverages of the surfaces and estimate the average island size in the overlayer. The results show the sensitivity of RHEED to the details of the island or step distribution on the surface. By comparing the AlAs and GaAs profiles it is apparent that Al is much less mobile on the (001) surface than is Ga. Finally we report the observation of surface roughening during the 2×4 to $c(4\times4)$ GaAs(001) phase transition.

I. INTRODUCTION

Reflection high-energy electron diffraction (RHEED) is extensively used to determine the periodicity and roughness of epitaxial films. Its natural compatibility with the growth of compound semiconductors by molecular-beam epitaxy (MBE) made it the standard *in situ* probe even though only qualitative information could be obtained. The purpose of this work is to analyze the shape of diffracted beams from GaAs and AlAs films deposited on GaAs(001) surfaces. We will show that the shapes of the RHEED beams that we measure agree with kinematic calculations[1] and can be used to follow the development of the microscopic surface morphology during epitaxial growth. Our emphasis here will be on the presence of random distributions of surface steps. These are of particular interest in crystal growth and dissolution phenomena because of their intrinsic self-regeneration property. The signature of surface steps in the diffraction pattern is a variation in the width of a diffracted beam (length of a RHEED streak) with a characteristic dependence on the angle of incidence. Similar dependencies are observed in low-energy electron diffraction experiments, though it is usually more convenient to vary the incident electron energy. An important difference is that our RHEED instrument can resolve order over about 10 000 Å, which is an order of magnitude greater than that resolvable by typical low-energy electron diffraction (LEED) instruments. We will measure the shape of the RHEED streaks as a function of angle of incidence. At certain angles, the diffraction from the tops and bottoms of steps are out of phase, resulting in maximal destructive interference and beam broadening. At other angles, the tops and bottoms of steps scatter in phase and the diffraction is insensitive to the step disorder. The main problem is to determine the distribution of steps giving rise to the particular shape measured. We recently analyzed the diffraction from a surface with a random distribution of steps.[1] For the case in which the scatterers were distributed among two layers the result was particularly simple: the diffracted beam profile could be written as the sum of a narrow central spike, reflecting the long-range order, and a broad function, dependent upon the form of the step disorder. For the case of a geometric distribution of steps,[1,2] a matrix method was used to show that the broad function was a Lorenztian whose width was related to the eigenvalues of the matrix describing the disorder. We showed that independent of the precise form of the step distribution, the relative contributions of the central spike and broadened part depended solely on the incident angle and the coverage (fraction of exposed surface atoms) on each level. The calculation was shown to agree with the LEED measurements of Gronwald and Henzler,[3] but insufficient data was available for a thorough test.

In what follows we present results of RHEED measurements of MBE prepared GaAs surfaces on which submonolayer amounts of GaAs and AlAs were deposited. The substrates were very flat and nearly singular so that these partial monolayer results can be compared to the simple two-level calculation. We will show that the sharp central spike and the step-broadened part are clearly evident. By fitting the measured diffracted beam profiles to calculations, the microscopic surface roughness of the deposited films will be characterized. We will demonstrate the sensitivity of RHEED to the details of the step distribution. The results will confirm the validity of our kinematic analysis.

II. EXPERIMENTAL

GaAs(001) substrates were prepared by MBE in a Perkin-Elmer MBE 400 system. One-micron buffer layers were grown on wafers that were first chemically etched and then cleaved into 4×5 mm sections. Details of the procedure have been described previously.[4–6] For the deposition of partial monolayers of GaAs, the sub-

strate was held at 450°C while the Ga shutter was opened for about 10 s with an excess As_4 flux present. Several short depositions were carried out until the diffraction was observed to change. The Ga flux correspond to a beam equivalent pressure of 1×10^{-9} Torr. Because of the possibility of an initial Ga burst, the time that the Ga shutter was open was not used to calibrate the deposition independently.

The diffraction measurements used a 10-keV electron gun at a glancing angle of the incidence between 2° and 4° and an angular divergence in the beam of 0.4 mrad. All measurements were made with the incident beam directed 7° from the [100] toward the [1$\bar{1}$0] direction in order to reduce the contribution of multiple scattering from other beams. Diffracted beam intensities were measured by focusing the light from the phosphor screen into an optical fiber which was connected to a photomultiplier. Profiles of the intensity along the length of the streak were obtained by magnetically translating the entire pattern across the fixed detector. The angles of incidence were found by measuring the distance between the straight-through beam and the specular beam and could be determined to within 1 mrad. Using the RHEED method of Pukite *et al.*,[5,6] the misorientation of the sample was determined to be less than 0.8 mrad.

After growth of the buffer layer the sample was annealed under the As_4 flux for about two hours at 580°C, the growth temperature. During this time the streaks that are observed during steady-state growth slowly contract into a semicircle of very sharp dots. The widths of the diffracted beams are then nearly instrument limited in both directions.[7] One should note that for the depositions to be studied here, the widths of the streaks parallel to the surface were always instrument limited and just equaled the range of angles in the incident beam. All of the profiles to be presented correspond to scans along the length of the streaks perpendicular to the surface. All GaAs depositions subsequent to the growth of the initial buffer layer were carried out at a substrate temperature of 450°C; at higher temperatures the step distributions would change substantially during the time required for the measurements.

III. RESULTS AND DISCUSSION

To demonstrate that a RHEED streak is composed of two parts, a central spike due to the long-range order over the surface and a broad function due to the step disorder, we need to measure the shape of a streak as a function of the incident angle, at a variety of coverages. Then for each coverage the angular dependence of the relative weighting of the two components can be compared to calculation. For a given coverage, the functional form of the step-broadened part must be the same at all angles—this function must be extracted to characterize the step distribution. We want to follow the development of this function as the coverage is increased to understand the mechanisms of epitaxial growth.

For these measurements the substrate temperature was sufficiently high that the deposited atoms could order, yet low enough to prevent diffusion across the long distances needed to change the distribution of steps during the time required for the measurements. Alternatively, rather than fix the coverage for many angular scans, as was done in these experiments, one could fix the angle and scan the diffracted beam during a continuous deposition.[4] This alternative method, though, lacks the control needed to compare scans taken at different incident angles.

To produce a static step distribution over the surface, several short depositions were made until broadening of the diffracted beam was observed at an out-of-phase angle. Then scans of the diffracted intensity as a function of final glancing scattering angle were measured for angles of incidence between 43 and 64 mrad. The results of one deposition, which best illustrates the expected diffraction from a two-level system, is shown in Fig. 1. The points shown correspond to data that has first been filtered by drawing a curve through the mean of the statistical noise from the weak signal and then digitized. The intensities are plotted against the angular deviation from the specular position. These intensities have been normalized to give the same value at the peak. The angle, θ_i, is the external glancing angle that the incident beam made with the sample surface and is not corrected for refraction by the crystal inner potential. No correction is made because the interference condition depends only on the extra external path length; a refraction correction at the top or bottom of a step would be identical and would cancel. The solid curve is a fit to the data to be described in Sec. IV.

The main feature to be noted at this point is the clear separation of the profile into a central spike that is present

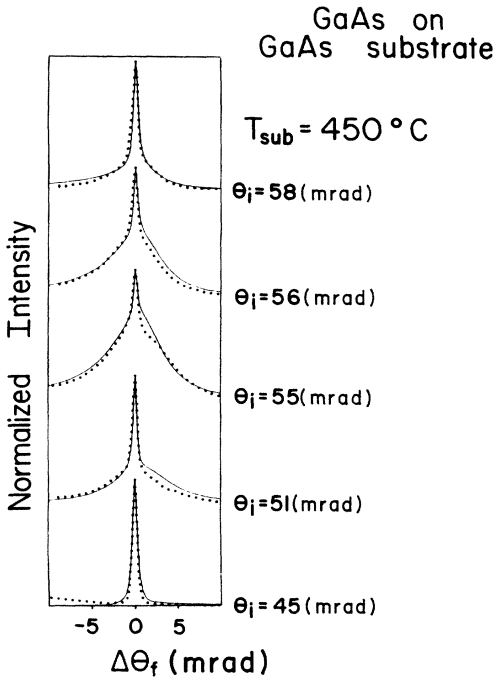

FIG. 1. Series of scans of the specular beam intensity at various incident angles after a brief deposit. The solid line is a fit using the analysis discussed in the text. The surface coverage is determined by the fit to be 0.5. The width of the step-broadened term corresponds to an average terrace length of about 300 Å.

at all angles and a broad part that changes with angle. This means that there are steps on the surface. For this two-level system, as will be seen later, it also means that the number of scatterers on each level is not equal. At 43 and 65 mrad, angles at which the interference from the top and bottom levels is constructive (Bragg angle), the diffraction is insensitive to the steps and the diffracted beam is as sharp as the range of angles in the incident beam. At intermediate angles the role of the destructive interference is evident, though importantly, the width of the broad function is unchanged. This variation in shape is distinctly different from what would be observed if the streaks were due to strain or a mosaic spread of small domains. Similar results were observed in the unique high-resolution LEED experiments of Gronwald and Henzler.[3]

The next series of measurements tests the analysis at different coverages and follows the development of the step-broadened component of the diffracted beam. A new sample was prepared as before and three depositions were made with the substrate at 450°C. After each deposition a series of scans of the specular beam was taken for a range of incident angles. The digitized results are shown in Figs. 2–4. The solid curves are fits to be described in Sec. IV. Once again there is a striking variation in the shape of the profiles as the interference condition between scattering from the tops and bottoms of the steps is unchanged.

An important difference between the data in Figs. 2–4

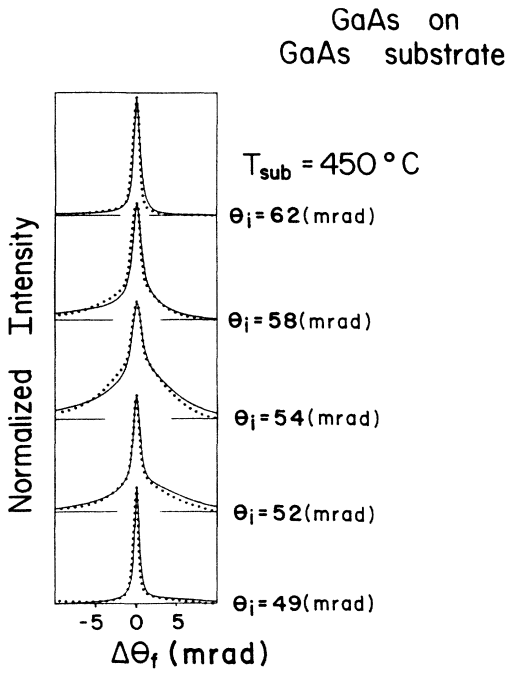

FIG. 3. Series of scans of the specular beam intensity at various incident angles after further growth. The solid line is a fit using the analysis discussed in the text. The surface coverage is determined by the fit to be 0.3. The width of the step-broadened term corresponds to an average terrace length of about 250 Å.

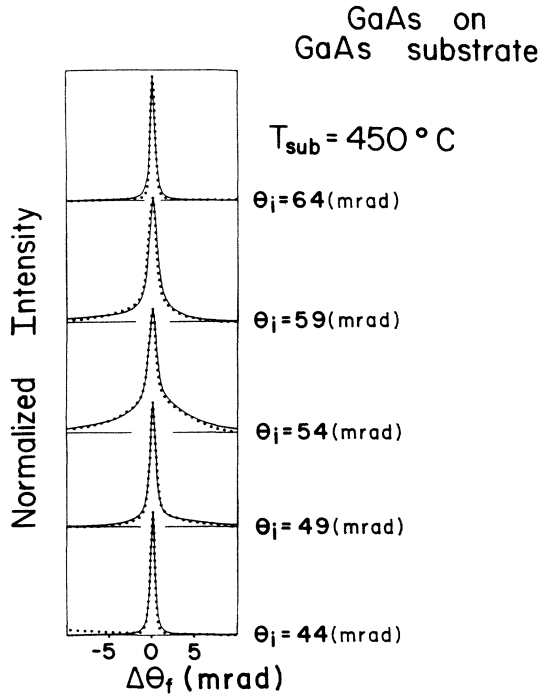

FIG. 2. Series of scans of the specular beam intensity at various incident angles after a brief deposit. The solid line is a fit using the analysis discussed in the text. The surface coverage is determined by the fit to be 0.2. The width of the step-broadened term corresponds to an average terrace length of about 250 Å.

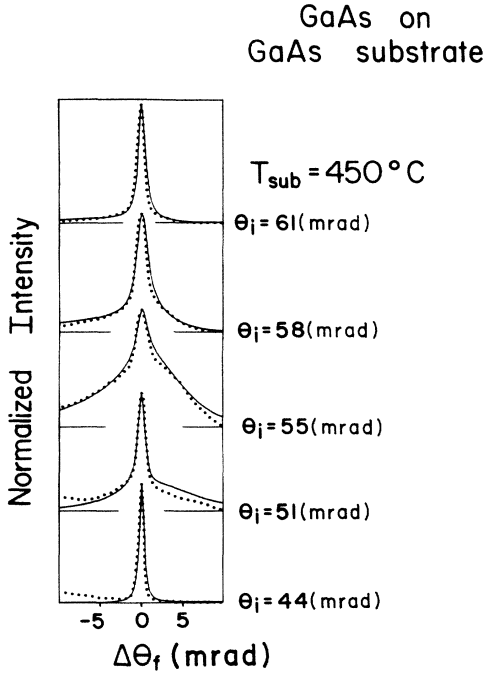

FIG. 4. A series of scans of the specular beam intensity at various incident angles after further growth. The solid line is a fit using the analysis discussed in the text. The surface coverage is determined by the fit to be 0.4. The width of the step-broadened term corresponds to an average terrace length of about 200 Å.

and that in Fig. 1 is the behavior of the central portion of the profiles as the angle of incidence is varied. In Figs. 2—4 the central spike is as sharp as permitted by instrument at the Bragg angles where the diffraction is insensitive to steps. Near the out-of-phase angle, however, it broadens significantly. This is in contrast to the data in Fig. 1 where the central spike remains sharp at all angles of incidence. To obtain the ideal behavior of Fig. 1 it is essential to prepare substrates that are atomically flat. There are two primary obstacles to this. First the crystal must be cut to be parallel with the low-index face to within a few tenths of a mrad; otherwise, the surface has a staircase of steps that are always present. Second the etching procedure must be carefully controlled to avoid introducing small ripples over the surface. This would give a macroscopic step distribution with large terrace lengths that are difficult to anneal away. Both of these can contribute to broadening of the central spike away from Bragg angles, as is observed in the second series of measurements.

More interestingly the data in Figs. 2—4 show that increasing the coverage of the overlayer decreases the mean terrace length or island size. As the coverage increases, the amount of broadening at out-of-phase angles of the wings of the profiles reflects the decrease in the correlation length over the surface.

To investigate the epitaxial growth of AlAs on GaAs, submonolayer amounts of AlAs were deposited on annealed GaAs substrates prepared as before except that the substrate temperature was maintained at the 580°C growth temperature throughout. Once again growth was terminated when a significant change in the diffraction pattern was observed. Scans of the specular beam were taken at various angles of incidence. These are shown in Fig. 5. Again, the results conform to the behavior expected. The broadened term, which is negligible at Bragg angles, becomes increasingly important as the angle of incidence approaches the out-of-phase condition. Very near the out-of-phase condition, the broad term dominates. Also, it should be noted that even though the substrate temperature was higher, the AlAs surface is rougher than the GaAs surface, the width of the broadened term being greater. The average terrace length is less than that of the GaAs surface and the distribution function of terraces is different. To remove this roughness, a higher-temperature anneal is needed. This indicates that the surface mobility of Al on GaAs is significantly less than that of Ga on GaAs. This result has been assumed by Singh and Bajaj[8] in Monte Carlo simulations of the growth of AlGaAs. One should also note that the separation between the central spike and the broad component of the diffracted beam is very clearcut. This is very much like the results reported by Gronwald and Henzler[3] and immediately indicates that the distribution of terraces is not geometric.[1]

The clean, annealed GaAs surface in each of the above cases exhibited the familiar arsenic-stabilized antiphase-disordered 2×4 reconstruction.[9] If the substrate temperature is lowered the reconstruction changes to a $c(4\times4)$ reconstruction. Beginning with a well-annealed surface, we slowly lowered the temperature and took scans of the specular beam at an angle of incidence corresponding to the out-of-phase condition where the diffraction pattern is most sensitive to steps. At the phase transition to the lower-temperature structure the sharp diffraction beam

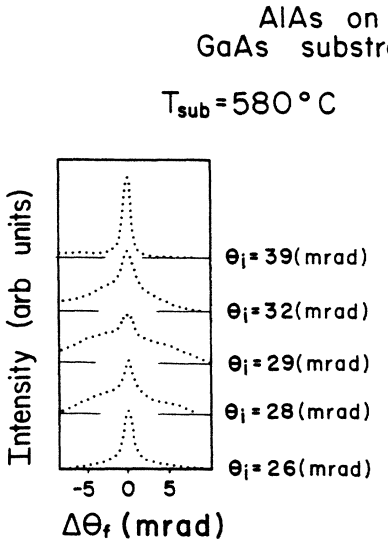

FIG. 5. Scans of the specular beam intensity after epitaxial growth of a small amount of AlAs on GaAs(001). Near 29 mrad, which is close to an out-of-phase angle, the profile is composed of two components: a central spike and a broad part. Away from this angle, the contribution of the broad part is much less than that of the central spike. For these low angles, the exact out-of-phase condition is shifted to about 29 mrad from 33 mrad. At the higher out-of-phase angles there is no shift (Ref. 19).

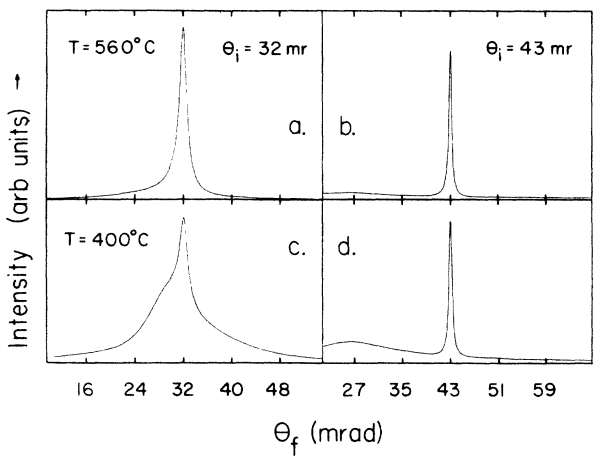

FIG. 6. Scans of the specular beam intensity of well-annealed GaAs(001). In (a) the angle of incidence is selected to be near the out-of-phase condition where diffraction is most sensitive to steps. Lowering the substrate temperature produces a phase transition to a different reconstruction accompanied by the appearance of a diffracted beam profile characteristic of surface steps. In (b), a Bragg angle, no change is observed. The increased background at lower scattering angles, θ_f, is the contribution from the out-of-phase angle.

suddenly developed the broadened base characteristic of surface step disorder. This is shown in Fig. 6(a). No change occurred at the in-phase angle, shown in Fig. 6(b), confirming that the change was indeed related to step formation on the surface. It has been shown[10] that the surface density of As for the lower-temperature reconstruction is higher than for the high-temperature reconstruction. Thus the appearance of steps may be a confirmation of Van Vechten's ideas[11] about the relief of density changes in phase transitions on surfaces by the formation of steps.

IV. ANALYSIS

We analyze the shapes of the diffracted beams described in Sec. III using the results of Ref. 1 for scattering from a surface with only two exposed levels. For GaAs prepared by molecular-beam epitaxy, we will demonstrate that scattering from surface steps dominates the reflection high-energy electron diffraction.

The diffracted intensity from a single beam, as a function of momentum transfer $\mathbf{S}=\mathbf{k}_f-\mathbf{k}_i$, can be written

$$I(\mathbf{S})=\left[A(\Theta,S_z)\left[\frac{2\pi}{a}\right]^2 N_0\delta(\mathbf{S}_{||})+B(\Theta,S_z)\left[\frac{N_0}{a^2}\right]F(\mathbf{S}_{||},\Theta)\right]\circ\mathscr{R}\ , \tag{1}$$

Here Θ is the coverage of the top layer and S_z and $\mathbf{S}_{||}$ are components of the momentum transfer perpendicular to and parallel to the surface. N_0 is the number of surface scatters. Convolution with an instrument response function, $\mathscr{R}$, is indicated. The coefficients A and B are defined as follows:

$$A(\Theta,S_z)=\Theta^2+(1-\Theta)^2+2\Theta(1-\Theta)\cos(S_z d)\ , \tag{2}$$

$$B(\Theta,S_z)=2\Theta(1-\Theta)[1-\cos(S_z d)]\ . \tag{3}$$

The function F depends on the details of the step distribution[1] and its normalization over all $\mathbf{S}_{||}$ follows that of Ref. 1. The function F is proportional to the Fourier transform of the pair correlation function, less a constant, between two sites on either the same level or on different levels. A measured RHEED profile at fixed incident angle could, very roughly, be considered a plot of the intensity given in Eq. (1), as a function of $\mathbf{S}_{||}$. Different values of the incident angle would correspond to different values of S_z.

The important variation to note is that for a given surface coverage, Θ, the disorder related function, F, is independent of S_z. At this time we lack a microscopic theory which would predict the exact form of the step distribution. Consequently, we can only determine whether a function F exists, giving the correct S_z dependence for the intensity profile. If such a function can be found, it must be step related. Our procedure is to select to a function F which has a minimum of free parameters and then to vary them to fit the data. We will exploit this general feature of the diffraction to measure the surface coverage.

The curves were fit using a Voigt profile for F. A Voigt profile is a convolution of a Lorenztian with a Gaussian. Aside from normalization there are two free parameters, the width of the Gaussian and the width of the Lorenztian. Fits with either of the component curves alone proved poor. An approximate form[12] was employed to speed calculation. In addition, a narrow Lorentzian instrument response function was used to reproduce the finite resolution of the diffractometer.

Two additional physical effects were included in the calculated intensity profiles: the atomic scattering factor and refraction. The diffracted intensity will vary along the length of the streak simply because the atomic scattering factor is varying with scattered angle. The scattering factor used in this calculation is that from arsenic (which differs very little from that for Ga) given by the Hartree-Fock calculation of Doyle and Turner.[13] The atomic scattering factor is determined by the scattering angle inside the crystal. The electrons are refracted by the inner potential of the solid both when they arrive at the surface and when they leave after scattering. The refracted glancing angle (inside the crystal) is given by

$$\theta_i^2\simeq\theta_0^2+\frac{V_I}{V}\ , \tag{4}$$

where θ_i and θ_0 are the refracted and unrefracted angles, respectively, V_I is the inner potential of 15.8 V,[14] and $V=10$ kV is the accelerating potential. Note that the phase shifts due to step interference occur outside the crystal so that refraction does not affect the angles of the Bragg and out-of-phase conditions.

The measured diffraction profiles were fit with curves generated from Eq. (1), using the atomic scattering factor that corresponds to the refracted scattering angles. Each set of profiles for different angles of incidence was fit simultaneously using a Simplex algorithm.[15] The width of the narrow central Lorentzian spike was allowed to vary with incident angle to account for a long-range waviness on the surface. This was necessary since a small macroscopic curvature is equivalent to a step distribution over many levels which cannot always be annealed out in the time scale of the experiment. Its effect is to slightly broaden the beam at the out-of-phase angle but is unaffected by the deposition. By allowing the width of the narrow central spike to vary, this macroscopic curvature is treated as an effective instrument response. The angle of incidence of each scan was allowed to vary by no more than 1 mrad to reflect the experimental uncertainty in this measurement. The two important parameters which were characteristic of the whole data set were the width of the broadened term and the surface coverage. Each Voigt profile has two characteristic widths but the smaller one, in this case the width of the Gaussian part, was set equal to the Lorentzian instrument response width. Note that one might have expected a Lorentzian step broadening convoluted with the measured Lorentzian instrument response. Instead, the Voigt profile used yielded better fits to the data. The width of the broad Lorentzian part of the Voigt profile was taken as a measure of the step disorder on the surface. Note that to do better one needs a complete microscopic picture of the disorder and that this procedure was chosen to show that the functional

TABLE I. Fitting parameters for Fig. 1. [Coverage $\Theta=0.47$; half width of broad Lorentzian, $b=9.9\times10^{-3}$ Å^{-1}, $L=\pi/b=320$ Å.]

θ_{inc} (mrad)	Half width of central spike (Å^{-1})
57.6	9.0×10^{-4}
55.6	7.6×10^{-4}
55.3	7.9×10^{-4}
51.1	5.9×10^{-4}
45.1	7.4×10^{-4}

TABLE III. Fitting parameters for Fig. 3. [Coverage $\Theta=0.28$; half width of broad Lorentzian, $b=1.4\times10^{-2}$ Å^{-1}, $L=\pi/b=230$ Å.]

θ_{inc} (mrad)	Half width central spike (Å^{-1})
61.8	1.4×10^{-3}
57.5	2.0×10^{-3}
54.4	1.9×10^{-3}
51.8	1.3×10^{-3}
48.5	8.3×10^{-4}

form of the intensity along a RHEED streak predicted by Eq. (1) is correct. The fits and the experimental data are shown in Figs. 1–4. The fitting parameters for Fig. 1 are shown in Table I. Tables II through IV show the fitting parameters for the three successive depositions of GaAs on GaAs of Figs. 2–4.

The tables also list the mean terrace separation length L associated with the width of each step-broadened term. This is simply taken to be 2π times the inverse of the width of the broadened term. It is the average distance between corresponding terrace edges on the surface, that is, the sum of average terrace length and the average "valley" length. This number is only approximate because the actual relation between the width of the diffracted profile and the mean terrace size depends specifically on the step distribution on the surface. Lu and Lagally[2] showed in numerical examples that the actual terrace size associated with a given width could vary by as much as a factor of 4 depending on the distribution assumed. Nevertheless, it is clear that the lengths of the terrace are many hundreds of angstroms.

The very long terrace lengths on the surface explain the success of the kinematic theory we have used in analyzing the data. Beam profiles can be analyzed with a kinematic theory provided two conditions are satisfied. First, the terraces on the surface must be long compared to the electron elastic mean free path of roughly 40 Å. The above discussion clearly demonstrates that the terrace lengths are much longer than this. Also, the angle of the diffracted beam must be such that the width of the scanned beam does not have contributions from too wide a range of S_z. The variation of intensity with S_z, caused by multiple scattering, was minimized in these experiments by choosing relatively high angles of incidence where the contribution from various S_z was minimal.

The quality of the fits shown confirms the ability of the kinematic approximation to account for the major contributions to the shapes of the diffracted profiles. Note that the data were not taken at conditions of high symmetry and that good fits were obtained at many incident angles. Multiple scattering is expected to change dramatically over the range of angles used; if it were significant it is unlikely that such a agreeement would have been obtained. An improvement which would take some multiple scattering effects into account is possible however. As mentioned before, due to the range of final scattering angles included when scanning over a diffracted beam, the profiles include diffraction from a range of values of S_z. Multiple scattering effects may cause variations in the diffracted intensity with S_z. An improvement to the fitting procedure used here would be to measure the intensity of the specular beam as a function of the angle of incidence and include this measured variation of intensity in the fitting calculations.[16] This would include empirically the major corrections to the kinematic results.

Other forms of disorder could also contribute to the broad component of the diffracted beam profile. For example, thermal diffuse scattering and even critical scattering in a phase transition give similar components that are distinct from the central spike. A point we wish to emphasize is that these other forms would not have the special dependence on S_z that is needed to explain these data from GaAs. Both after deposition of submonolayers as well as for exceedingly smooth surfaces with unavoidable slight macroscopic undulations, the data presented have this special dependence. Thus unlike suggestions that

TABLE II. Fitting parameters for Fig. 2. [Coverage $\Theta=0.22$; half width of broad Lorentzian, $b=1.2\times10^{-2}$ Å^{-1}, $L=\pi/b=220$ Å.]

θ_{inc} (mrad)	Half width central spike (Å^{-1})
63.5	9.9×10^{-4}
58.6	1.7×10^{-3}
53.8	1.5×10^{-3}
49.2	9.4×10^{-4}
43.6	6.4×10^{-4}

TABLE IV. Fitting parameters for Fig. 4. [Coverage $\Theta=0.36$; half width of broad Lorentzian, $b=1.6\times10^{-2}$ Å^{-1}, $L=\pi/b=200$ Å.]

θ_{inc} (mrad)	Half width central spike (Å^{-1})
60.7	1.6×10^{-3}
58.4	2.5×10^{-3}
54.7	2.2×10^{-3}
50.7	1.3×10^{-3}
44.4	7.6×10^{-4}

thermal diffuse scattering is the dominant cause of RHEED streaks,[17,18] our results indicate that even from exceedingly smooth GaAs surfaces prepared by MBE, steps are the primary contributor.

V. SUMMARY

Submonolayer amounts of GaAs and AlAs were deposited onto GaAs(001) substrates at 450 °C in order to create a simple two-level surface. The angular profiles of the specular, reflection high-energy electron diffraction beam were measured for each coverage at different incident angles. The measured profiles of these two-level systems show a clear separation into a central spike due to the long-range order over the surface and also a broad function due to the disorder. The profiles were fit to a single-scattering (column approximation) calculation for a two-level system. The results demonstrate that the disorder component is predominantly determined by the steps on the surface. A Voigt profile was used to model the step disorder and to estimate the correlation lengths for GaAs. Preliminary work on AlAs showed it to have a smaller average terrace length. By fitting the calculation to the measured profiles, the surface coverages were determined, RHEED may finally begin to be considered a quantitative method.

ACKNOWLEDGMENTS

This work was supported in part by the Ceramics Program of the National Science Foundation (NSF) Grant No. DMR-83-19821, by the University of Minnesota Center for Microelectronics and Information Sciences, and by the Corrosion Center of the University of Minnesota (supported by U.S. Department of Energy Contract No. DOE/DE-FG02-85ER45173). We are grateful to P. R. Pukite and J. M. Van Hove for helpful discussions and their assistance in collecting the data. We especially want to thank P. R. Pukite for critically reviewing this manuscript.

---

*Present address: Department of Physics, University of Notre Dame, Notre Dame, IN 46566.

[1]C. S. Lent and P. I. Cohen, Surf. Sci. **139**, 121 (1984).
[2]T.-M. Lu and M. G. Lagally, Surf. Sci. **120**, 47 (1982).
[3]K. D. Gronwald and M. Henzler, Surf. Sci. **139**, 180 (1982).
[4]J. M. Van Hove, P. R. Pukite, and P. I. Cohen, J. Vac. Sci. Technol. B **3**, 563 (1985).
[5]P. R. Pukite, J. M. Van Hove, and P. I. Cohen, Appl. Phys. Lett. **44**, 456 (1984).
[6]P. R. Pukite, J. M. Van Hove, and P. I. Cohen, J. Vac. Sci. Technol. B **2**, 243 (1984).
[7]J. M. Van Hove, P. R. Pukite, P. I. Cohen, and C. S. Lent, J. Vac. Sci. Technol. A **1**, 609 (1983).
[8]J. Singh and K. K. Bajaj, J. Vac. Sci. Technol. B **2**, 576 (1984).
[9]J. M. Van Hove, P. I. Cohen, and C. S. Lent, J. Vac. Sci. Technol. A **1**, 546 (1983).
[10]P. Drathen, W. Ranke, and K. Jacobi, Surf. Sci. **77**, L162 (1978).
[11]J. A. Van Vechten, J. Cryst. Growth **38**, 139 (1977).
[12]J. Puerta and P. Martin, Appl. Opt. **20**, 3923 (1981).
[13]P. A. Doyle and P. S. Turner, Acta Crystallogr. **24**, 390 (1968).
[14]P. R. Pukite, M. S. E. E. Thesis, University of Minnesota, 1983 (unpublished).
[15]J. A. Nelder and R. Mead, Computer J. **7**, 308 (1965); M. Caceci and W. Caceris, Byte 9(5), 340 (1984).
[16]P. R. Pukite, C. S. Lent, and P. I. Cohen, Surf. Sci. **161**, 39 (1985).
[17]S. Holloway and J. L. Beeby, J. Phys. C **11**, L247 (1978).
[18]B. K. Argawal, Phys. Rev. B **30**, 4412 (1984).
[19]P. I. Cohen, P. R. Pukite, J. M. Van Hove, and C. S. Lent, J. Vac. Sci. Technol. (to be published).